Reaction Mechanisms

International Edition: DOI: 10.1002/anie.201601049
German Edition: DOI: 10.1002/ange.201601049

Analyzing the Case for Bifunctional Catalysis

*Mie Andersen, Andrew J. Medford, Jens K. Nørskov, and Karsten Reuter**

Abstract: *Bifunctional coupling of two different catalytic site types has often been invoked to explain experimentally observed enhanced catalytic activities. We scrutinize such claims with generic scaling-relation-based microkinetic models that allow exploration of the theoretical limits for such a bifunctional gain for several model reactions. For sites at transition-metal surfaces, the universality of the scaling relations between adsorption energies largely prevents any improvements through bifunctionality. Only the consideration of systems that involve the combination of different materials, such as metal particles on oxide supports, offers hope for significant bifunctional gains.*

The discovery of scaling relations between the adsorption energies of atomic and molecular species on transition-metal surfaces has greatly advanced our theoretical understanding of catalysis in recent years.[1–3] This descriptor-based approach, relying only on the adsorption energies of a few key reaction intermediates, has proven highly instrumental in rationalizing why often only few catalyst materials meet the narrow range of binding energies that allow the dissociation of reactants without hindering the formation of products.[4] There is a long-standing and widespread hope that these severe limitations in material space could be overcome by bifunctional catalysts, which couple two different active-site types, each catalyzing a particular reaction step.[5–7]

Herein, we focus on the diffusional coupling between active sites located in spatially distinct regions. Such spillover mechanisms have been proposed between metal particles and metal supports[8,9] or, more commonly, between metal particles and non-metal supports.[10–12] In the spirit of developing an understanding of trends and limitations, the present work employs descriptor-based approaches to generally assess the performance gains that are possible through diffusive coupling. To this end, we consider two generic reaction schemes that are rate-limited by one adsorption and one reaction/desorption step. Eq. (1) describes the adsorption of a species A onto a single active-site type s:

$$A(\mathrm{g}) + {}^*_s \rightleftharpoons A_s \tag{1}$$

whereas Eq. (2) considers an adsorption process leading to two reaction intermediates on the surface:

$$AB(\mathrm{g}) + 2{}^*_s \rightleftharpoons A_s + B_s \tag{2}$$

In both cases, the initial step is followed by an associative reaction/desorption step, either only

$$2A_s \rightleftharpoons 2{}^*_s + A_2(\mathrm{g}) \tag{3}$$

in the case of Eq. (1), or additionally

$$2B_s \rightleftharpoons 2{}^*_s + B_2(\mathrm{g}) \tag{4}$$

in the case of Eq. (2). If A(g) represents a solvated proton and electron and A_2(g) represents H_2(g), Eq. (1) and (3) directly describe the hydrogen evolution reaction (HER). Similarly, if AB(g) represents NO(g), A_2(g) represents N_2(g), and B_2(g) represents O_2(g), Eq. (2)–(4) describe NO decomposition. Under suitable assumptions concerning the rate-limiting steps, more complex reaction schemes can also be mapped onto these conceptual ones. The overall conclusions derived from our study of these two reaction schemes do not depend on the scheme or the specific reaction conditions (temperature and gas-phase pressure) investigated and are therefore expected to have fairly general implications for the concept of bifunctionality as a whole.

A summary of the microkinetic models and the choice of reaction parameters are given in Section S1 in the Supporting Information. Most importantly, the activation energy of an individual reaction step, E^{act}, is assumed to scale linearly with the reaction energy, ΔE, according to the Brønsted–Evans–Polyani (BEP) relation:

$$E^{\mathrm{act}} = \alpha^* \Delta E + \beta \tag{5}$$

The use of BEP relations allows the entire dependence on the actual catalyst used to be contained in typically only one to two free parameters (or descriptors). For the first reaction scheme (Eq. (1) and (3)), this is the adsorption energy of the reaction intermediate A, E^A_s, whereas for the second reaction scheme (Eq. (2)–(4)), the adsorption energy of reaction intermediate B, E^B_s, is additionally included. We consider a range between −4 eV (strongly exothermic adsorption) and up to +4 eV (strongly endothermic adsorption) for these parameters, such that plots of the turnover frequency (TOF) as a function of these adsorption energies will lead to the well-known volcano plots in the monofunctional case.

[*] Dr. M. Andersen, Prof. Dr. K. Reuter
Chair for Theoretical Chemistry and Catalysis Research Center
Technische Universität München
Lichtenbergstrasse 4, 85747 Garching (Deutschland)
E-mail: karsten.reuter@ch.tum.de
Dr. A. J. Medford, Prof. J. K. Nørskov, Prof. Dr. K. Reuter
SUNCAT Center for Interface Science and Catalysis
Department of Chemical Engineering, Stanford University
Stanford, CA 94305 (USA)
Dr. A. J. Medford, Prof. J. K. Nørskov, Prof. Dr. K. Reuter
SUNCAT Center for Interface Science and Catalysis
SLAC National Accelerator Laboratory
2575 Sand Hill Road, Menlo Park, CA 94025 (USA)
Supporting information and the ORCID identification number(s) for the author(s) of this article can be found under http://dx.doi.org/10.1002/anie.201601049.

The dependence on the explicit reaction described through these Equations as well as the geometrical facet of the catalyst is contained in the BEP parameters α and β. These parameters have been computed for a wide range of reactions.[13] On transition metals, they are surprisingly universal, showing only small variations for different classes of reactions and over different metal facets.[14,15] For example, dehydrogenation steps typically have final-state-like transition states with α values close to 1, whereas A–A and A–B bond-breaking reactions show α values in the range of 0.5–0.9. The β parameters for metals are mostly found in the range of 1–2 eV and can be rather sensitive to the geometric structure of the metal facet. Typically, open surfaces have lower β values for A–A and A–B bond-breaking reaction steps than close-packed surfaces, whereas hydrogenation reactions in most cases show the opposite trend, though much less pronounced. Support materials are often made out of transition-metal oxides, which have been shown to obey scaling relations that are different from those on metals.[16–18] The range of α and β values is nevertheless similar to the one described for metals.

To describe a bifunctional catalyst, we extend the reaction schemes to two hypothetical site types s and t. The coupling between the two monofunctional catalysts then takes place as a result of the diffusion of intermediates, for example for A:

$$A_s + {}^*_t \rightleftharpoons {}^*_s + A_t \qquad (6)$$

The plausibility of bifunctional activity gains through such coupling steps is thereby assessed in two ways: 1) a gain relative to the sum of the activities of the two considered decoupled catalysts (hereafter denoted as relative bifunctional gain) and 2) a gain relative to the activity of two sites on the optimal monofunctional catalyst (hereafter denoted as absolute bifunctional gain).

We first address bifunctionality for the case where both site types exhibit identical BEP parameters. This situation would, for example, apply to the literature case of a metal particle on a metal support,[8,9] assuming that no important geometrical difference in site type exists between particle and support. We consider only the difference in adsorption energy between the two sites as a thermodynamic barrier for the diffusion step. Any resulting bifunctional gain is then an upper limit as compared to the situation with additional kinetic diffusion barriers.

Figure 1 a shows the resulting TOF maps for the coupled and decoupled case, as well as the corresponding relative bifunctional gain for the first reaction scheme (Eq. (1) and (3)), when specifically using BEP parameters representative for the HER on a (111) metal facet from Ref. [19]. In the decoupled case, the variation of the adsorption energy of A

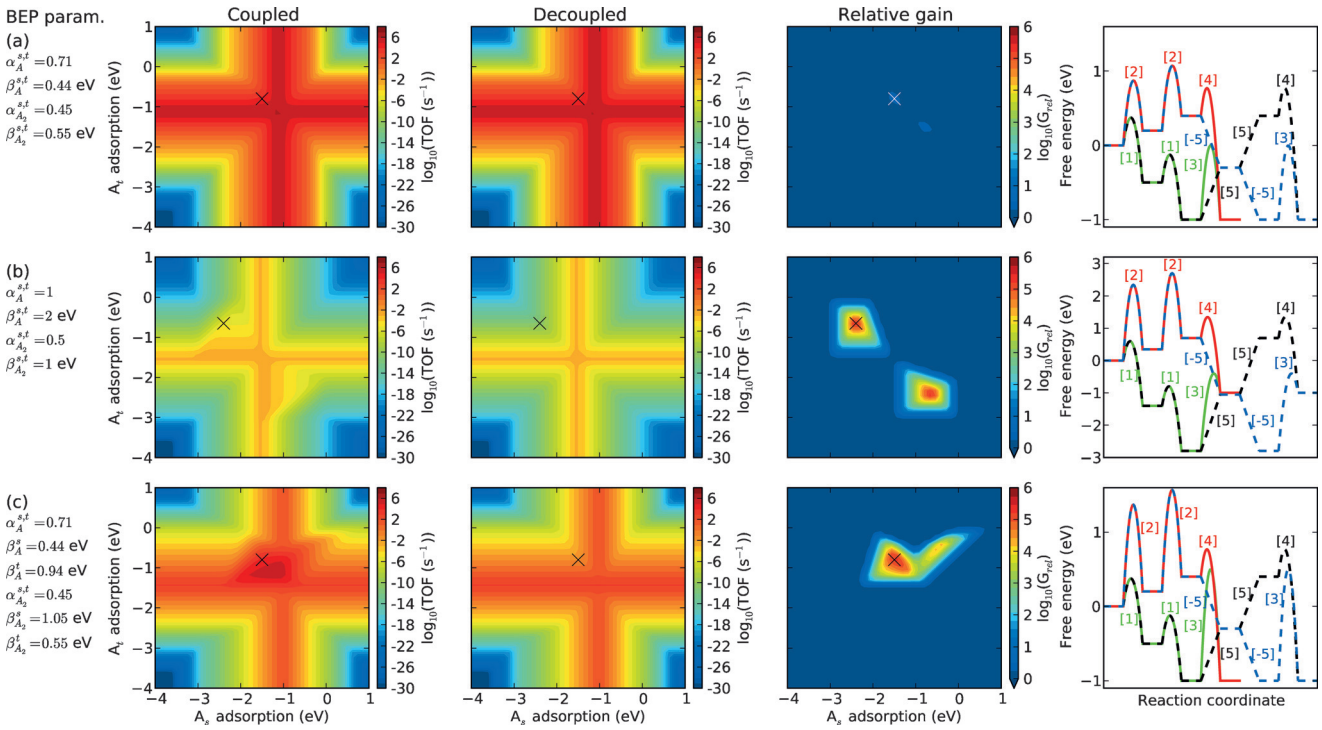

Figure 1. TOF maps for the bifunctionally coupled (left) and decoupled (center left) reaction scheme shown in Eq. (1) and (3), the relative bifunctional gain, G_{rel} (center right), defined as the ratio of the coupled to the decoupled TOF, as well as the free energy diagram for the point marked with an X in the TOF maps (right). In the diagrams, the decoupled pathways on the reactive s site (green solid line), the noble t site (red solid line), and the endergonic (black dashed line) and exergonic (blue dashed line) diffusion pathways are shown. The numbers refer to the individual reaction steps: [1] and [2]: Adsorption of A on s and t sites, respectively. [3] and [4]: Desorption of A_2 on s and t sites, respectively. [5] and [−5]: Diffusion of A from an s to a t site and from a t to an s site, respectively. The three cases correspond to a) identical BEP parameters on the two sites representative for the HER on a (111) metal facet, b) identical BEP parameters on the two sites corresponding to the largest relative bifunctional gain found when varying the BEP parameters, and c) different BEP parameters on the two sites, where the β value for A_2 desorption (A adsorption) on the s (t) site has been raised by 0.5 eV with respect to the parameters representative for the HER. The values of the BEP parameters used in each case are indicated to the left.

gives rise to identical one-dimensional volcano plots for the *s* and *t* sites, where too weak binding (very noble site) or too strong binding (very reactive site) of *A* leads to low TOFs. Intriguingly, this is hardly changed through the introduction of the diffusional coupling step, that is, the coupled case leads to a TOF map that is completely identical to the decoupled one, except for a tiny relative bifunctional gain at the point marked with an X (see also the identical symmetry-related gain on the opposite side of the diagonal, which is not hidden by the X). The far right panel in Figure 1 a shows the free energy diagram for the two decoupled and two diffusion-coupled pathways at this point in descriptor space. The tiny gain arises from the endergonic diffusion pathway shown in black. There are two requirements for obtaining a bifunctional gain from this pathway: First, the rate-limiting step on the reactive *s* site must be A_2 desorption, whereas on the noble *t* site, it must be *A* adsorption. Only in this case can the coupled pathway, which avoids both of these steps, give rise to a larger rate than achieved by any of the two decoupled catalysts individually. Second, the diffusion step must not limit the rate of the coupled pathway with respect to the decoupled pathways, that is, $E_t^A - E_s^A$ cannot be too high. The failure to simultaneously fulfill these two requirements is what limits the gain to the tiny area of descriptor space in Figure 1 a.

To generalize this concept to other reactions, we stick to identical BEP parameters for the two sites, but let the values vary within the ranges observed for real reactions as outlined in Section S2. Figure 1 b summarizes the results for those BEP parameters for which the highest relative bifunctional gain was identified in this search. It is seen that a relative gain of up to a factor of 10^5 is now possible in certain areas of descriptor space. Again, the gain arises from the endergonic diffusion pathway, which for these special values of BEP parameters has a maximal efficiency with low energy barriers for *A* adsorption on the reactive *s* site and A_2 desorption from the noble *t* site, as compared to *A* adsorption on the noble *t* site and A_2 desorption from the reactive *s* site. This is generally the case for large α values. Low BEP α parameters can also give rise to concomitant bifunctional gains (not shown), which then arise from the exergonic diffusion pathway. However, in both cases, these special values of the BEP parameters are at the boundaries of the values observed for real reactions. On top of this, as seen in Figure 1 b, the largest relative gains are limited to areas of descriptor space where the TOF for the decoupled catalyst is already extremely low, in this case only about 10^{-10} s^{-1}. Thus the practical catalytic relevance of such relative gains is expected to be low as the absolute catalytic activity of the coupled catalyst system is still far inferior to the optimum monofunctional catalyst.

For the second reaction scheme (Eq. (2)–(4)), we qualitatively obtained the same findings as for the first reaction scheme (Eq. (1) and (3)). Figure 2 shows the TOF maps and the relative bifunctional gains when specifically using the BEP parameters representative for NO decomposition on a metal(111) facet.[20] Even though huge relative bifunctional gains can again be found towards the extreme regions of descriptor values, they nevertheless still correspond to an insignificant absolute catalytic activity (compare the left and middle panels). We note that our findings are expected to hold also for high coverages where lateral interactions become significant, as such interactions typically do not change the BEP relations, but merely lead to a shift in the adsorption energies.

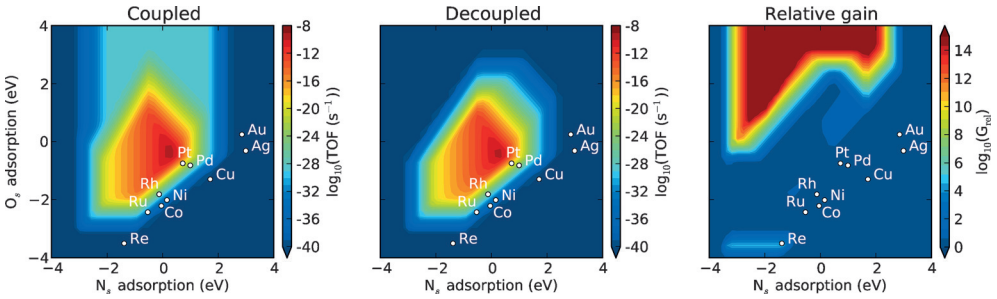

Figure 2. Coupled (left) and decoupled (center) TOF maps and the relative bifunctional gain, G_{rel}, (right) for the reaction scheme shown in Eq. (2)–(4) using BEP parameters and a reaction enthalpy representative for NO decomposition on a metal(111) facet from Ref. [20]. For the adsorption energies on the *t* site, values representative for Ag were used.

From the analysis to this point, the real virtue of bifunctionality could at best arise from catalysts exhibiting two site types that do not follow the same BEP relations. This could be the case for sites located on different geometric facets of a metal particle, or one site could be located on a metal particle and the other site on a non-metal support material. However, not just any difference in the BEP parameters will result in a gain. Analogously to the special values of BEP parameters behind Figure 1 b, the difference in BEP parameters between the two sites should favor one reaction step on the *s* site and another reaction step on the *t* site. The most effective way of obtaining this is by introducing a difference in the BEP β parameters in an opposite fashion on the two sites: $\Delta\beta = \beta_A^s - \beta_A^t = \beta_{A_2}^t - \beta_{A_2}^s$. Figure 1 c illustrates this for $\Delta\beta = 0.5$ eV, that is, the β value for A_2 desorption (*A* adsorption) on the *s* (*t*) site has been raised by 0.5 eV. The maximum relative bifunctional gain obtained for this case is roughly similar to the gain obtained with identical (special) BEP parameters on the two sites (compare Figure 1 b, c). However, in Figure 1 c, the gain is now located near the area of maximum catalytic activity of the decoupled catalyst, meaning that in this case an absolute bifunctional gain relative to the decoupled catalyst is achieved. Such gains are therefore much more interesting than those observed for identical BEP parameters on the two sites. In the illustrated case for $\Delta\beta = 0.5$ eV, the absolute bifunctional gain is around a factor of 600. The gain is observed to grow roughly exponentially with the value of $\Delta\beta$ (not shown), as the β value

adds directly to the activation barrier for the reaction step. An absolute bifunctional gain can also be achieved by modifying the BEP α parameters (see Figure S1). However, we find the effect of varying the α parameters within the ranges observed for real reactions to be much smaller than the effect of varying the β parameters.

Having generically established that an opposite variation in the BEP β parameters is the most effective way of achieving an absolute bifunctional gain, we proceeded to consider an explicit example where this required variation is found on different facets of transition-metal surfaces, namely ammonia synthesis combining (211) steps with (111) terraces. Here, the β value for N–N bond breaking is 0.56 eV lower on the step, whereas the β values for the hydrogenation steps are between 0.29 eV and 0.42 eV lower on the terrace.[15,20] Figure 3 shows the TOF maps and the bifunctional gain

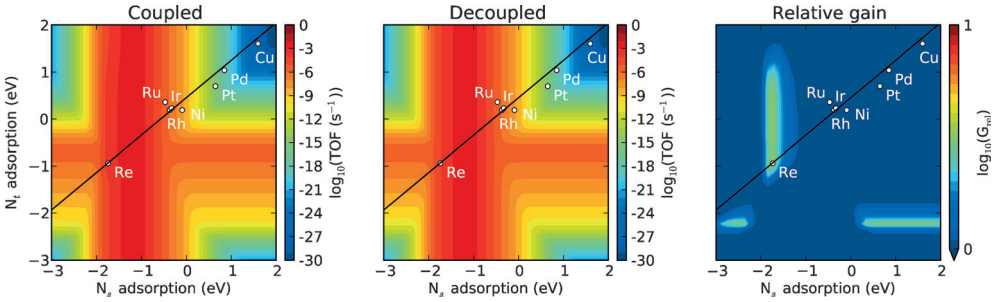

Figure 3. Coupled (left) and decoupled (center) TOF maps and the relative bifunctional gain, G_{rel} (right), for ammonia synthesis, coupling a metal(211) (*s* site) and a metal(111) (*t* site) facet. The adsorption energies of N on various metals define the scaling relation between adsorption on the two facets (black line), which would act as a constraint in the case where the two catalytic sites are composed of the same metal or alloy.

resulting from a detailed microkinetic model employing these parameters and considering diffusional coupling between the two facets (see also Section S3). The absolute bifunctional gain found for this system is only about a factor of 1.1 and therefore much lower than the gain found for the model reaction. On both sites, the rates of the decoupled pathways are predominantly controlled by N_2 splitting (high descriptor values), and only for $E_s^N < -1.2$ eV and $E_t^N < -2$ eV, they are controlled by a hydrogenation step (NH_2 hydrogenation). Furthermore, for $E_s^N < -1.2$ eV, the endergonic diffusion pathway, which gives rise to the absolute bifunctional gain by diffusion of N from the *s* to the *t* site, becomes rate-limited by the diffusion step. This means that the areas of descriptor space where the two sites have a different rate-limiting step and where the bifunctional efficiency is not limited by the diffusion step (which, as discussed above, is a requirement for achieving even a relative bifunctional gain) are also very limited (Figure 3). In the model reaction in Figure 1c, in contrast, the areas of descriptor space with different rate-limiting steps are much larger, which allows for much larger relative (and absolute) bifunctional gains. This illustrates that large gains can be achieved only if the BEP parameters are different enough to significantly change the rate-determining step between the two site types. Specifically, this must occur in areas of descriptor space where the bifunctional gain is not diminished by the diffusion step.

Even though ammonia synthesis is an example showing some of the largest variations in BEP parameters with site types on metal surfaces, the differences between step and terrace sites are apparently not pronounced enough to lead to significant gains. It thus seems that a combination of different materials such as metals and oxides is required to really make the case of bifunctionality. This is consistent with multiple claims in the literature on systems that exploit both diffusion (spillover) pathways and sites at the interface between metal particles and oxide supports. For oxides, only very limited information on BEP parameters is available. Ref. [17] gives the BEP relations for the reaction steps involved in NO decomposition on rutile and perovskite surfaces. However, the coupling of metals with either of these transition-metal oxides does not result in the required opposite variation in the BEP parameters: The BEP β values are smaller for all reaction steps on the oxides. As expected, no bifunctional gain can then be achieved (not shown). This demonstrates that a combination of different materials is a necessary, but not sufficient condition to invoke bifunctionality as an explanation for enhanced catalytic activity.

In conclusion, we have employed generic scaling-relation-based microkinetic models to investigate diffusionally coupled bifunctional catalysts. As long as the bifunctionality involves active-site types obeying identical BEP parameters, we generally find that gains occur only for particular BEP parameters and, even then, only in uninteresting areas of low catalytic activity. The true value of bifunctionality only emerges when two sites with largely different BEP parameters are coupled. For such cases, potentially involving sites at a metal nanoparticle and an oxide support, our analysis predicts that huge absolute gains in catalytic activity are possible in principle. However, our results also demonstrate that any coupling of materials obeying different BEP parameters is not sufficient for such a gain. The parameters must vary in a way that makes one reaction step most favorable on one site type and another reaction step most favorable on the other site type. This is achieved most effectively by an opposite variation of the BEP β parameters on the two site types. The BEP parameters must thereby be different enough to generate significantly different rate-limiting steps on the two sites, specifically also in areas of descriptor space where the diffusion step is favorable enough to allow for a bifunctional gain.

Acknowledgements

M.A. acknowledges funding from the Alexander von Humboldt foundation. A.J.M. is grateful for support through the

National Defense Science and Engineering Graduate Fellowship (NDSEG) program of the Department of Defense.

Keywords: bifunctional catalysis · computational chemistry · diffusion · reaction mechanisms · transition metals

How to cite: *Angew. Chem. Int. Ed.* **2016**, *55*, 5210–5214
Angew. Chem. **2016**, *128*, 5296–5300

[1] F. Abild-Pedersen, J. Greeley, F. Studt, J. Rossmeisl, T. R. Munter, P. G. Moses, E. Skúlason, T. Bligaard, J. K. Nørskov, *Phys. Rev. Lett.* **2007**, *99*, 016105.
[2] F. Calle-Vallejo, D. Loffreda, M. T. M. Koper, P. Sautet, *Nat. Chem.* **2015**, *7*, 403–410.
[3] J. K. Nørskov, T. Bligaard, B. Hvolbaek, F. Abild-Pedersen, I. Chorkendorff, C. H. Christensen, *Chem. Soc. Rev.* **2008**, *37*, 2163–2171.
[4] J. K. Nørskov, T. Bligaard, J. Rossmeisl, C. H. Christensen, *Nat. Chem.* **2009**, *1*, 37–46.
[5] A. Vojvodic, J. K. Nørskov, *Natl. Sci. Rev.* **2015**, *2*, 140–149.
[6] J. Saavedra, H. A. Doan, C. J. Pursell, L. C. Grabow, B. D. Chandler, *Science* **2014**, *345*, 1599–1602.
[7] G. Germani, Y. Schuurman, *AIChE J.* **2006**, *52*, 1806–1813.
[8] S. Pandelov, U. Stimming, *Electrochim. Acta* **2007**, *52*, 5548–5555.
[9] L. Wang, U. Stimming, M. Eikerling, *Electrocatalysis* **2010**, *1*, 60–71.
[10] R. Prins, *Chem. Rev.* **2012**, *112*, 2714–2738.
[11] G. N. Vayssilov, G. P. Petrova, E. A. I. Shor, V. A. Nasluzov, A. M. Shor, P. S. Petkov, N. Rosch, *Phys. Chem. Chem. Phys.* **2012**, *14*, 5879–5890.
[12] H.-Y. T. Chen, S. Tosoni, G. Pacchioni, *ACS Catal.* **2015**, *5*, 5486–5495.
[13] J. S. Hummelshøj, F. Abild-Pedersen, F. Studt, T. Bligaard, J. K. Nørskov, *Angew. Chem. Int. Ed.* **2012**, *51*, 272–274; *Angew. Chem.* **2012**, *124*, 278–280.
[14] S. Wang, B. Temel, J. Shen, G. Jones, L. Grabow, F. Studt, T. Bligaard, F. Abild-Pedersen, C. H. Christensen, J. K. Nørskov, *Catal. Lett.* **2011**, *141*, 370–373.
[15] S. Wang, V. Petzold, V. Tripkovic, J. Kleis, J. G. Howalt, E. Skulason, E. M. Fernandez, B. Hvolbaek, G. Jones, A. Toftelund, H. Falsig, M. Bjorketun, F. Studt, F. Abild-Pedersen, J. Rossmeisl, J. K. Nørskov, T. Bligaard, *Phys. Chem. Chem. Phys.* **2011**, *13*, 20760–20765.
[16] E. M. Fernández, P. G. Moses, A. Toftelund, H. A. Hansen, J. I. Martínez, F. Abild-Pedersen, J. Kleis, B. Hinnemann, J. Rossmeisl, T. Bligaard, J. K. Nørskov, *Angew. Chem. Int. Ed.* **2008**, *47*, 4683–4686; *Angew. Chem.* **2008**, *120*, 4761–4764.
[17] A. Vojvodic, F. Calle-Vallejo, W. Guo, S. Wang, A. Toftelund, F. Studt, J. I. Martinez, J. Shen, I. C. Man, J. Rossmeisl, T. Bligaard, J. K. Nørskov, F. Abild-Pedersen, *J. Chem. Phys.* **2011**, *134*, 244509.
[18] F. Vines, A. Vojvodic, F. Abild-Pedersen, F. Illas, *J. Phys. Chem. C* **2013**, *117*, 4168.
[19] E. Skúlason, V. Tripkovic, M. E. Björketun, S. Gudmundsdóttir, G. Karlberg, J. Rossmeisl, T. Bligaard, H. Jónsson, J. K. Nørskov, *J. Phys. Chem. C* **2010**, *114*, 18182–18197.
[20] H. Falsig, J. Shen, T. S. Khan, W. Guo, G. Jones, S. Dahl, T. Bligaard, *Top. Catal.* **2014**, *57*, 80–88.

Received: February 1, 2016
Published online: March 23, 2016

